

Supporting Information

Nanostructural Evolution of Natural Rubber/Silica Nanoparticle Coagulation from Binary Colloidal Suspensions to Composites: Implications for Tire Materials

Gianluca Cattinari^{1*}, *Karine Steenkeste*¹, *Sandrine Lévêque-Fort*¹, *Clément Cabriel*¹, *Ariane Deniset-Besseau*², *Alexis Canette*³, *Julian Oberdisse*⁴, *Matthieu Gallopin*⁵, *Marc Couty*⁵, *Marie-Pierre Fontaine-Aupart*¹

¹ Université Paris-Saclay, CNRS, Institut des Sciences Moléculaires d'Orsay, 91405, Orsay, France

² Université Paris-Saclay, CNRS, Institut Chimie Physique (LCP), 91405, Orsay, France

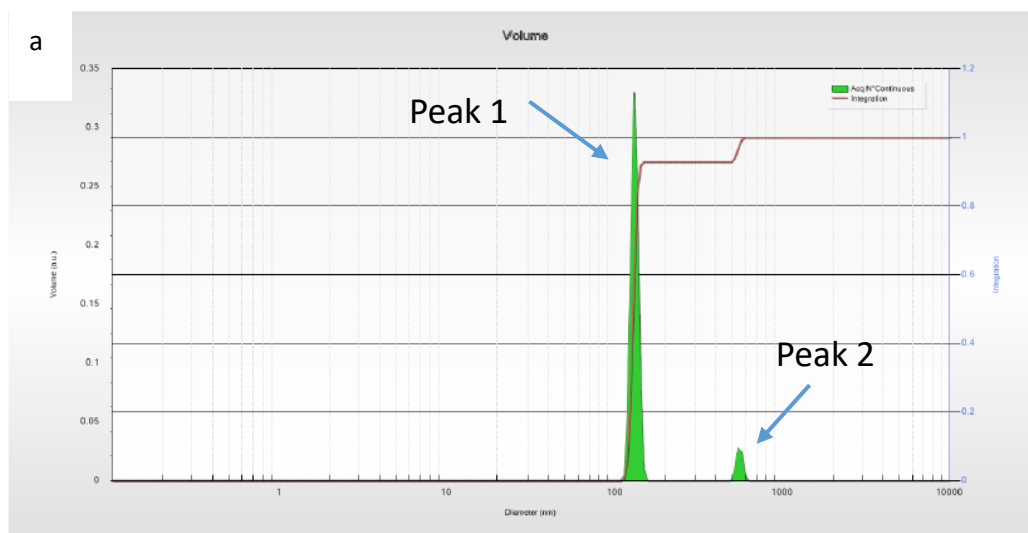
³ Sorbonne Université, CNRS, Institut de Biologie Paris-Seine (IBPS), Service de microscopie électronique (IBPS-SME), F-75005, Paris

⁴ Laboratoire Charles Coulomb (L2C), Université de Montpellier, CNRS, F-34095 Montpellier, France

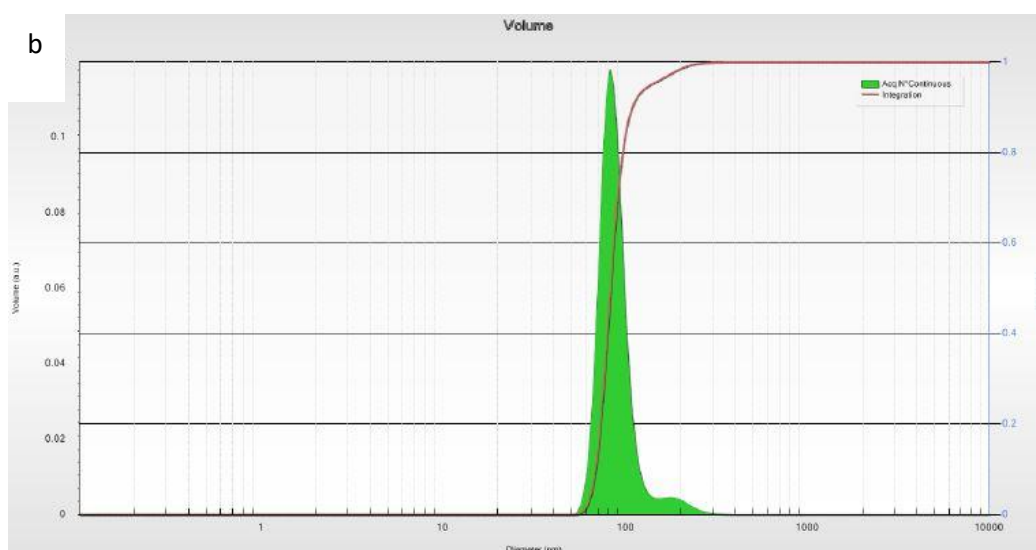
⁵ Manufacture Française des Pneumatiques MICHELIN, 23, place des Carmes-Déchaux 63000, Clermont Ferrand, France

* E-mail: gianluca.cattinari@u-psud.fr/gianluca.cattinari@michelin.com

Figure S1. DLS measurement of (a) NR particles (0.075 wt%) and (b) Silica nanoparticles (SiO_2NPs) recorded using a DLS Cordouan Vasco Flex apparatus. The particle size and distribution are based on volume.



Peak1	Mean: 130,60 nm	Std Dev: 6,29%	Intensity: 92,9%
Peak2	Mean: 554,27 nm	Std Dev: 5,59%	Intensity: 7,1%



Peak1	Mean: 86 nm	Std Dev: 18	Intensity: 96%
Peak2	Mean: 180 nm	Std Dev: 19	Intensity: 4%

Figure S2. SE micrograph on NR latex (without Mg^{2+} ions) at the end of 10 oscillation cycles of shear. The NR globular structure is maintained attesting that the shear conditions used does not induce any NR structural deformation on the NR globules in absence of Mg^{2+} ions. Magnification 10000x.

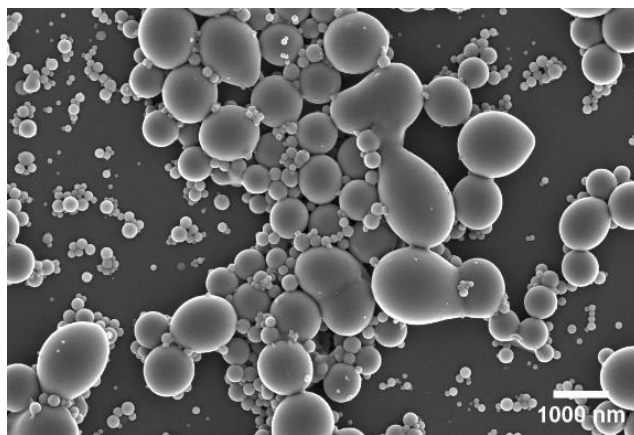


Figure S3. Fluorescence absorption and emission spectra of the involved fluorophores. Absorption (dashed line) and emission (full line). 532nm and 633nm inserted line represent the respective excitation with the laser. Cy5-NHS is the fluorophore used to label proteins, while either Dil or DID were used as lipid probes. SiO₂NPs were commercially labeled and no indication on the type of fluorophore was given by the manufacturer (Kisker Biotech, Germany).

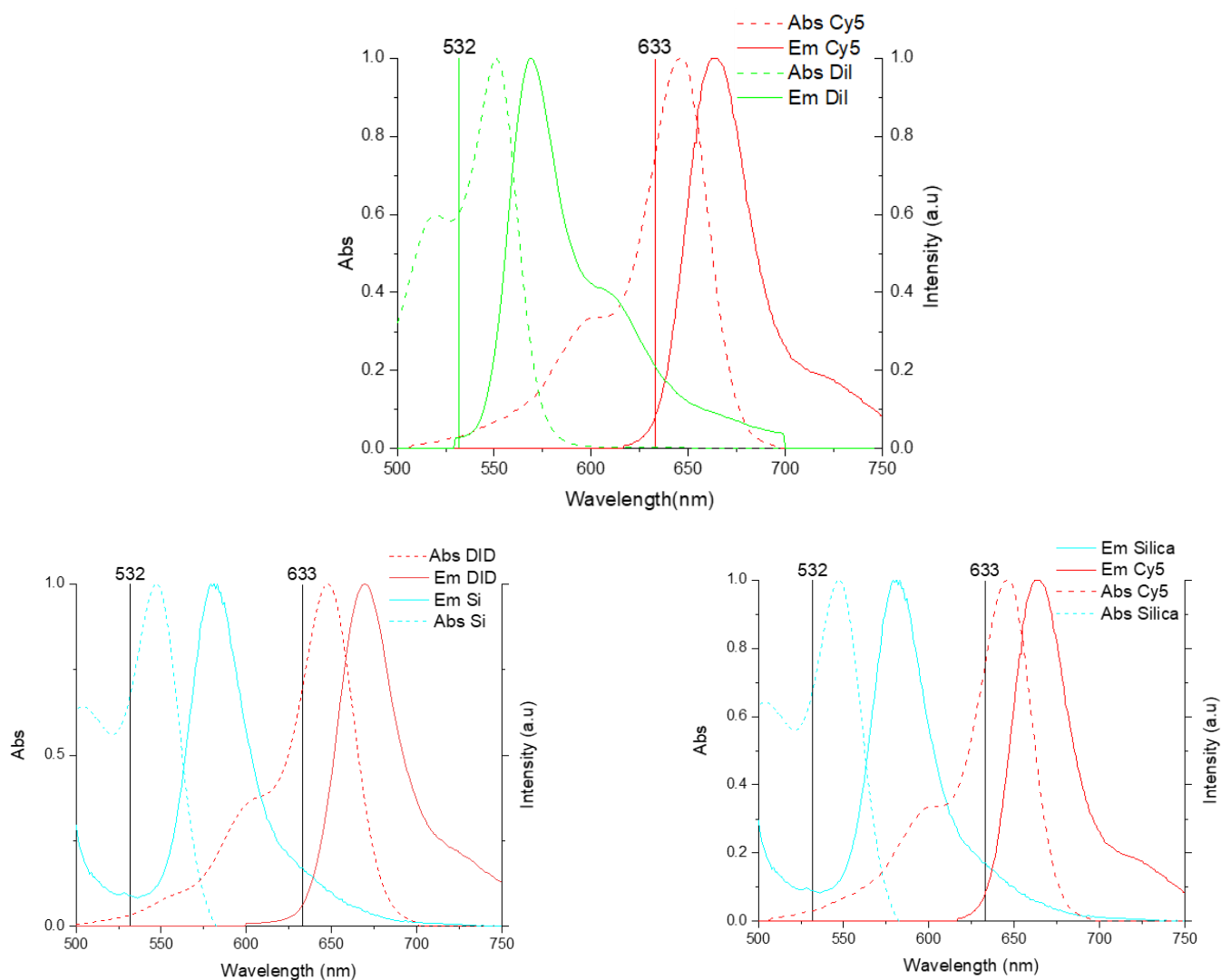


Figure S4. Fluorescence emission spectra of SiO₂NPs in absence and presence of Cy5 and Dil.

Recorded by Cary Eclipse (Varian, Palo Alto, CA, USA).

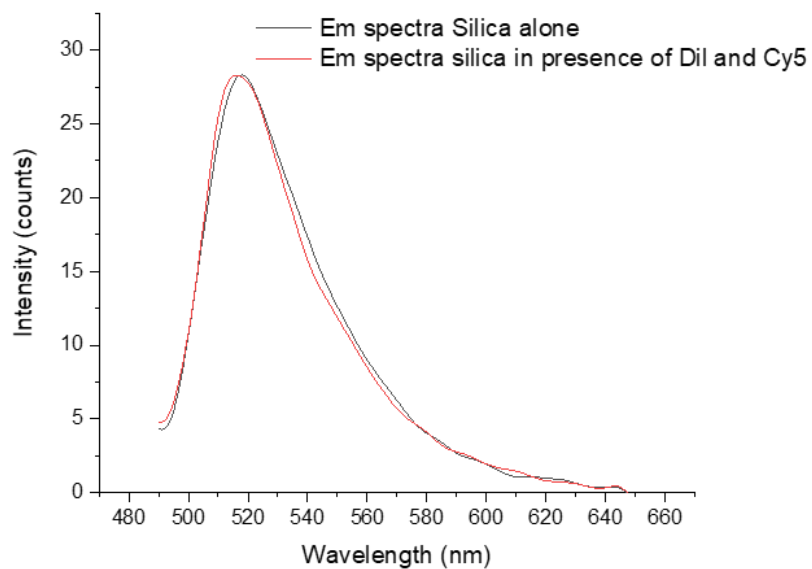


Figure S5. Large view SE image of the NR-SiO₂NPs composite formed on a Ibidi correlative support for CLEM experiments combining FESEM and d-STORM acquisitions on to different microscopy set-up.

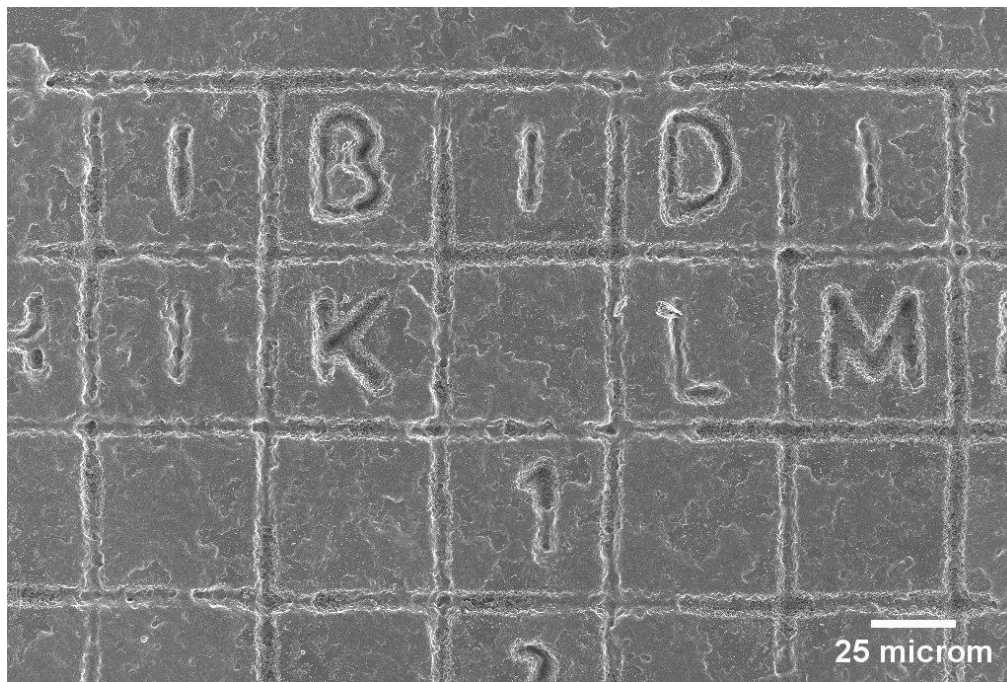


Figure S6. (a) SE and (b) BSE micrographs of the NR-SiO₂NPs hetero-aggregate obtained in presence of Mg²⁺ ions (100 mM ionic strength); structure fixed at t=1 h.

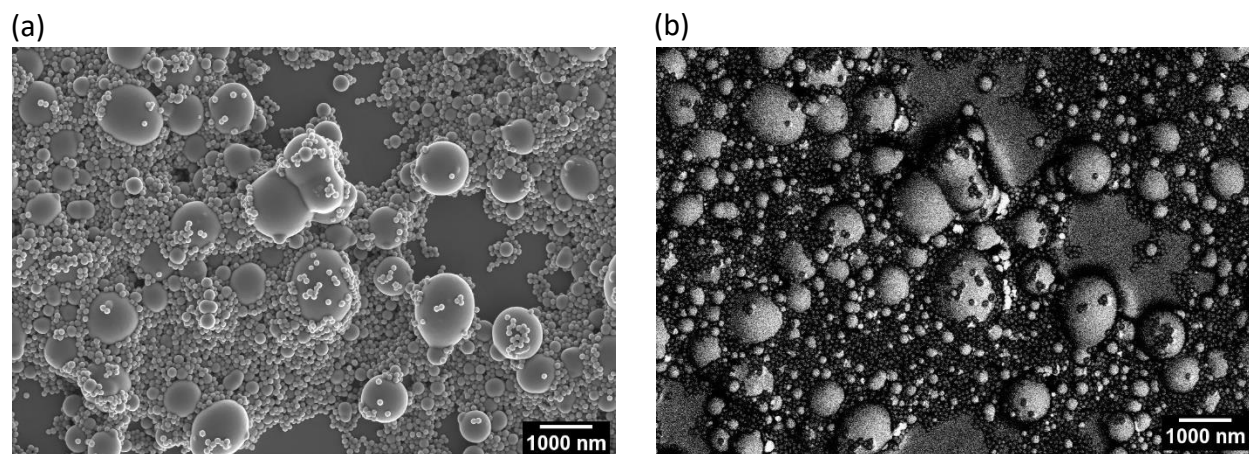


Figure S7. Light transmission images recorded along with shearing oscillation cycles for the NR-SiO₂NPs binary colloidal suspension in presence (a) and absence of ionic medium (b). Mechanical forces were applied using the RheOptiCAD module. The parameters of each oscillation correspond to 10 Hz frequency; total displacement of 1 μm displacement; 500 μm of gap; and 60s of application. The application of shear favors the quick formation of a hetero-aggregate. Images have been acquired using an Olympus 60x water immersion objective having 1.1 N.A and a CCD camera (UCBO, Olympus). Scale bar corresponding to 10 μm .

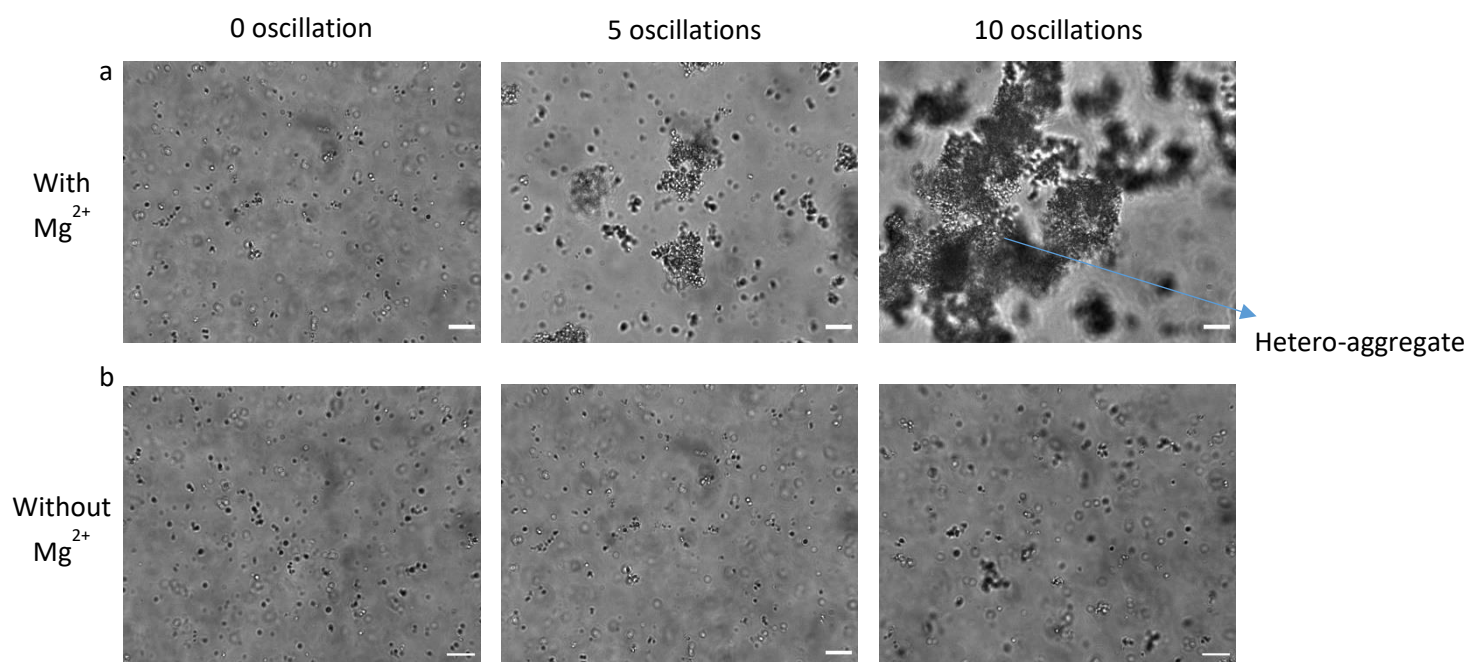


Figure S8. FTIR absorption spectra of (a) NR and (b) SiO₂NPs acquired in ATR mode and displayed in the range of 1800-900 cm⁻¹.

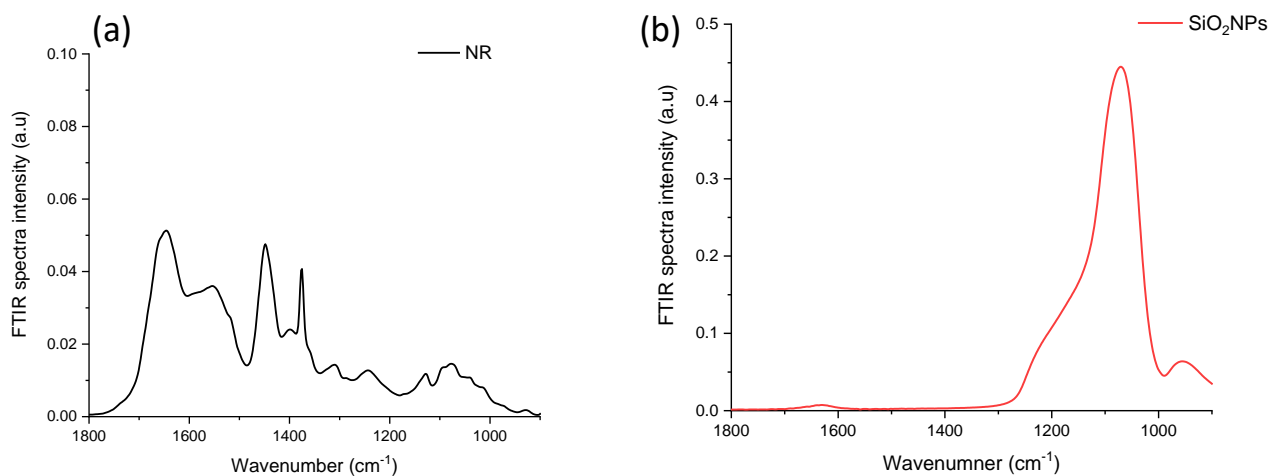


Figure S9. SiNPs distribution in the NR- SiO₂NPs composite (t=24 h) obtained after post-mixing shear application. AFM (a) height image. (b) IR map at 1100 cm⁻¹ of the corresponding region referring to Si-O-Si asymmetric stretching. The circled areas highlight a specific arrangement of SiO₂NPs in ellipse-ring like structures. (c) IR map at 1450 cm⁻¹ referring to the CH₂ bending.

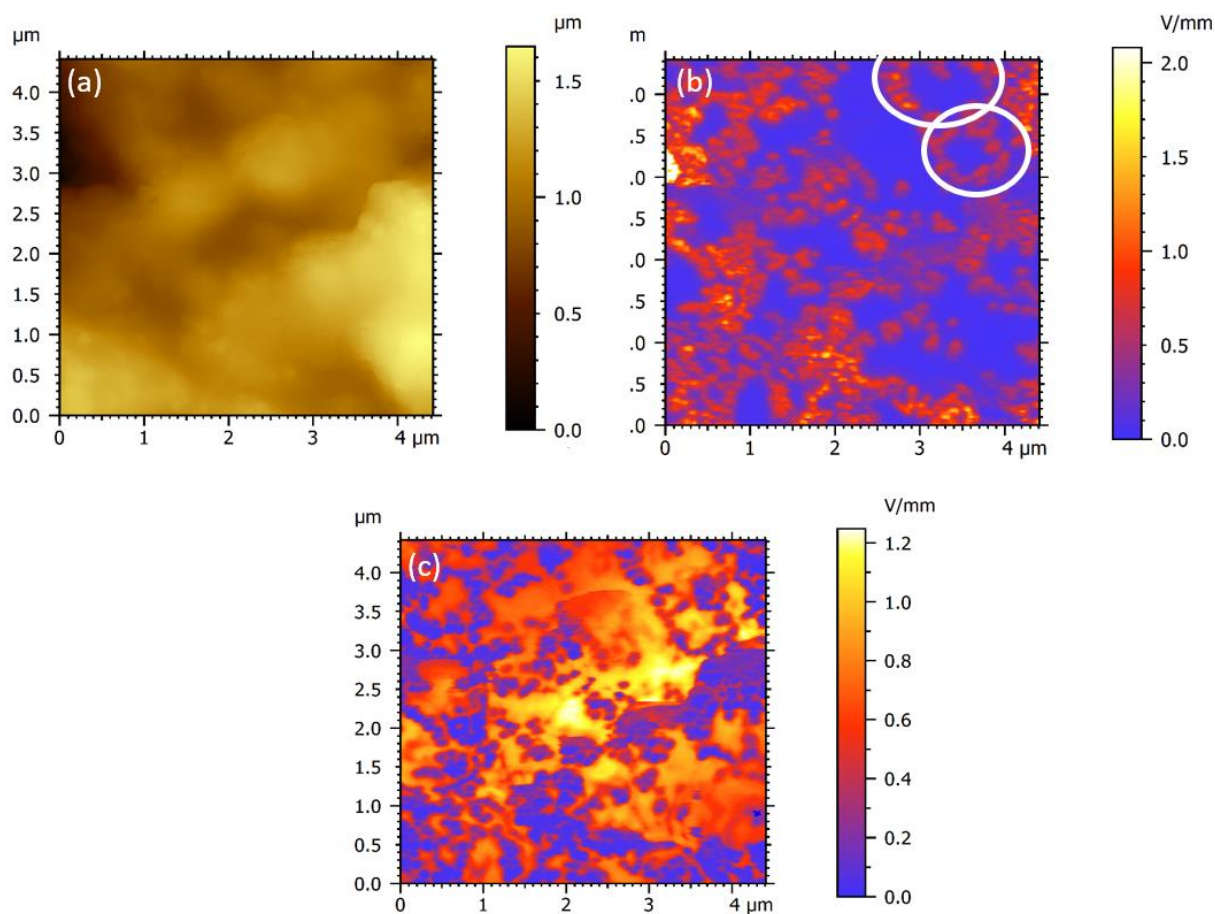


Figure S10. DBSCAN cluster analysis run on ROI regions of the d-STORM images corresponding to proteins in the NR-SiO₂NPs composite and the NR film. (a and b) d-STORM ROI and DBSCAN detection of protein clusters in the NR-SiO₂NPs composite. (c and d) d-STORM ROI and DBSCAN detection of proteins clusters in the NR matrix in absence of SiNPs. DBSCAN parameters: $\epsilon=50\text{nm}$ and $\text{MinPts}=50$. The analysis shows a marked clustering of proteins in the NR-SiO₂NPs composite. Image size ($10\text{ }\mu\text{m} \times 10\text{ }\mu\text{m}$).

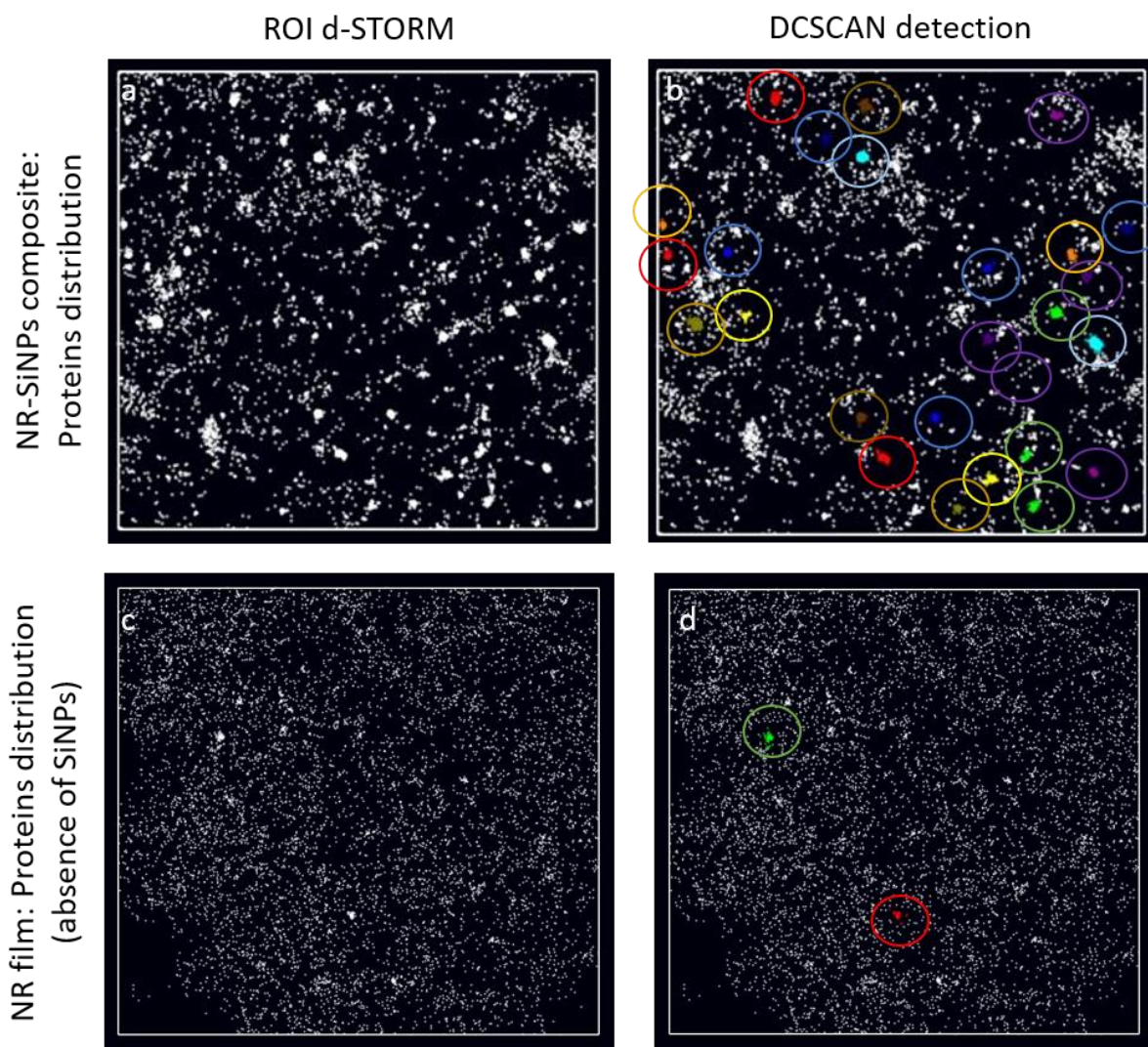


Figure S11. DBSCAN cluster analysis run on ROI regions of the d-STORM images corresponding to lipids in the NR-SiO₂NPs composite and the NR film. (a and b) d-STORM ROI and DBSCAN detection of lipid clusters in the NR-SiO₂NPs composite. (c and d) d-STORM ROI and DBSCAN detection of proteins clusters in the NR matrix in absence of SiO₂NPs. DBSCAN parameters: $\epsilon=50\text{nm}$ and $\text{MinPts}=50$. The analysis shows clustering of lipid in the NR-SiO₂NPs composite. Image size ($10\text{ }\mu\text{m} \times 10\text{ }\mu\text{m}$).

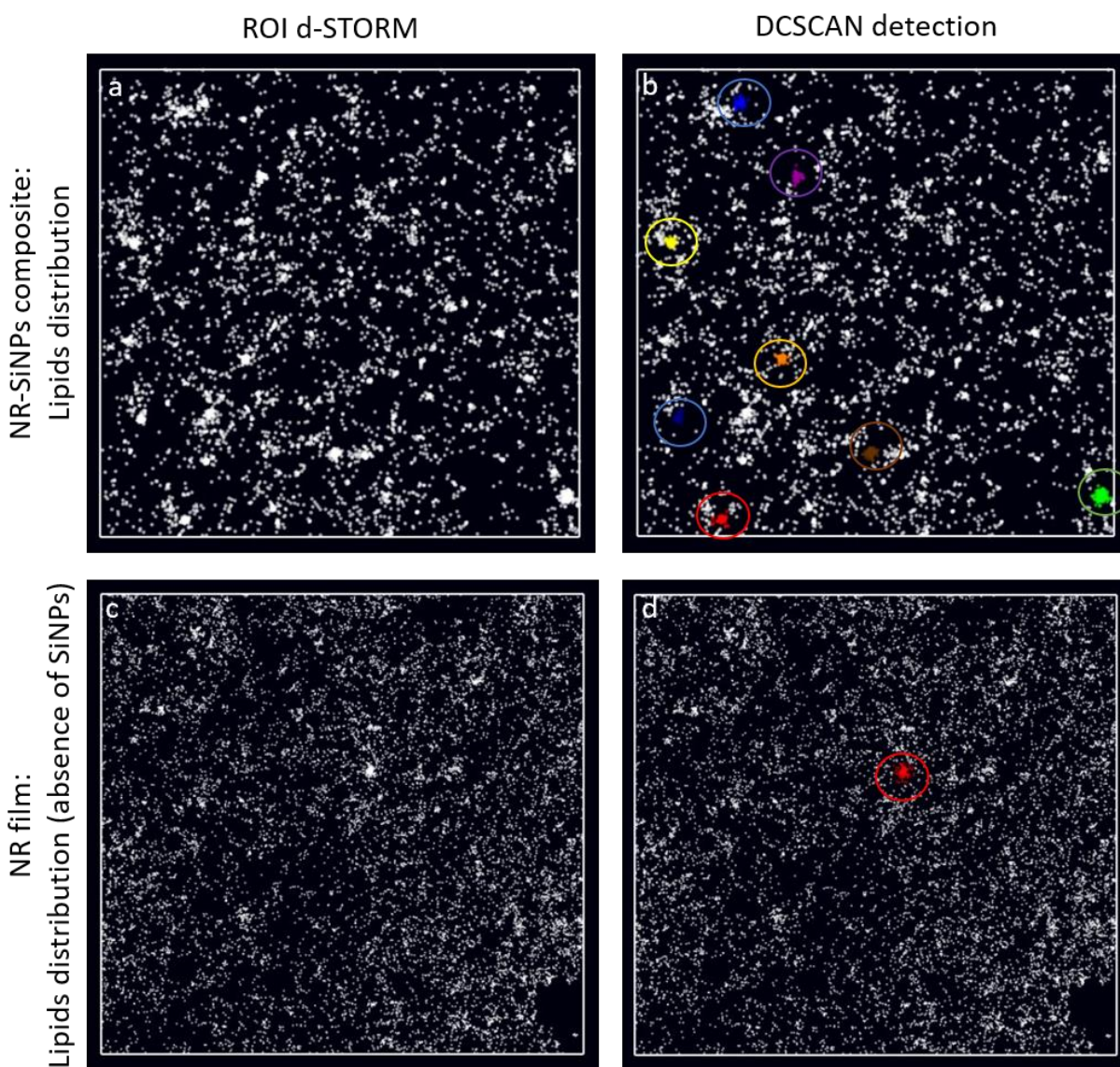


Figure S12. Distribution of proteins and lipids in NR-SiO₂NPs hetero-aggregate at t=4 h, when the solvent is majorly evaporated. Images acquired using total internal reflection fluorescence (TIRF) as excitation mode. (a) Dual color d-STORM fluorescence image of proteins (red) and lipids (green) showing the organization of the bio-molecules into clustered domains. Yellow circles in (a) highlight circular form corresponding to leftover globular forms. Pair-correlation analysis of lipids (b) and proteins (c) for the hetero-aggregate at t= 4 h (□), and comparison with results obtained for the NR-SiO₂NPs composite (■).

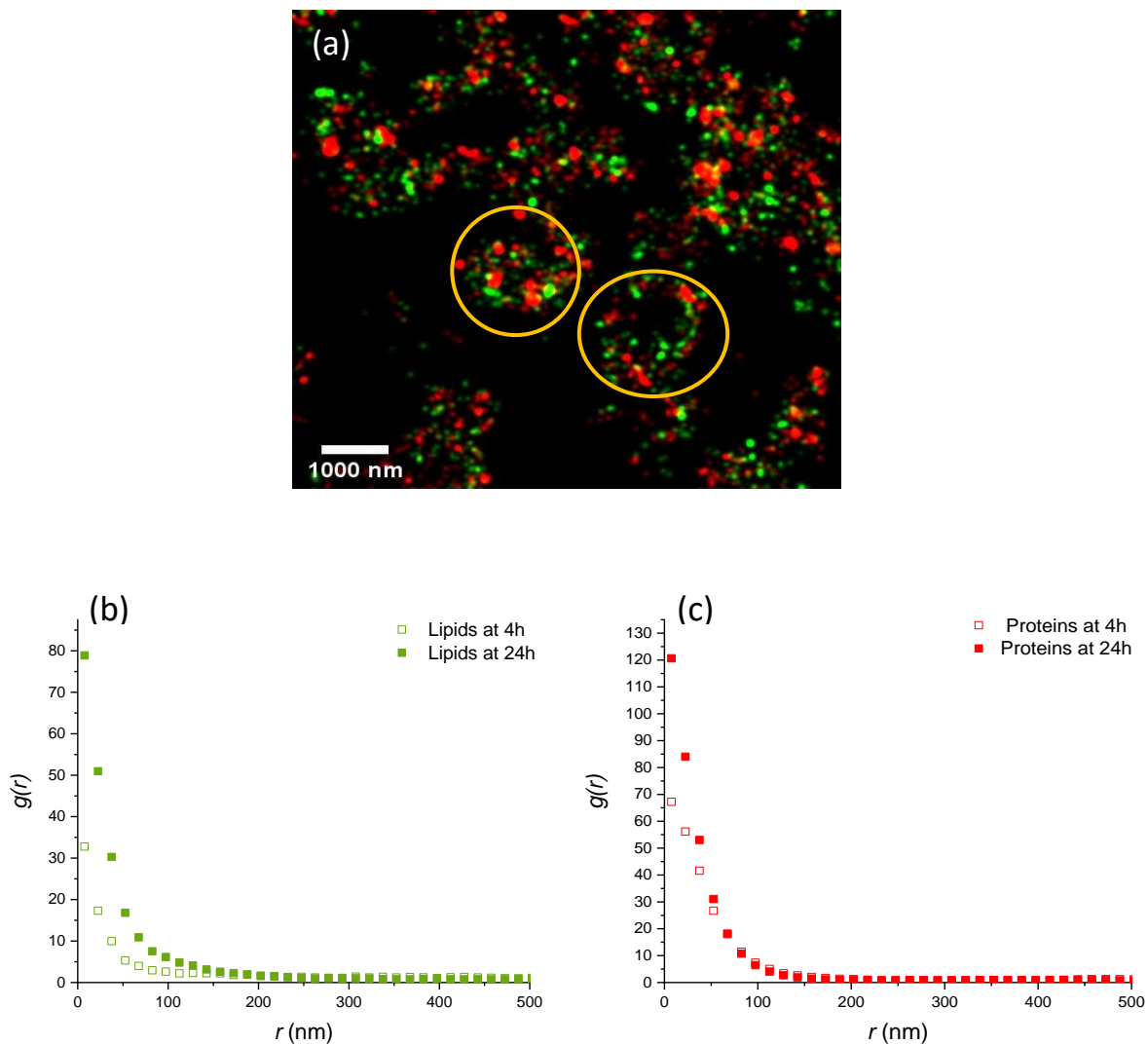


Figure S13. Distribution of proteins and lipids in NR-SiO₂NPs film formed in absence of the ionic medium, at t=24h. (a) Epifluorescence image (EPI). (b) Dual color d-STORM fluorescence image of proteins (red) and lipids (green) of the same zone. (c) Magnified view of the boxed region in b (image size: ~10 x 10μm). Pair-correlation analysis of lipids (d) and proteins (e) for the NR matrix in absence of SiO₂NPs (□), and comparison with results obtained for the NR-SiO₂NPs composite (■).

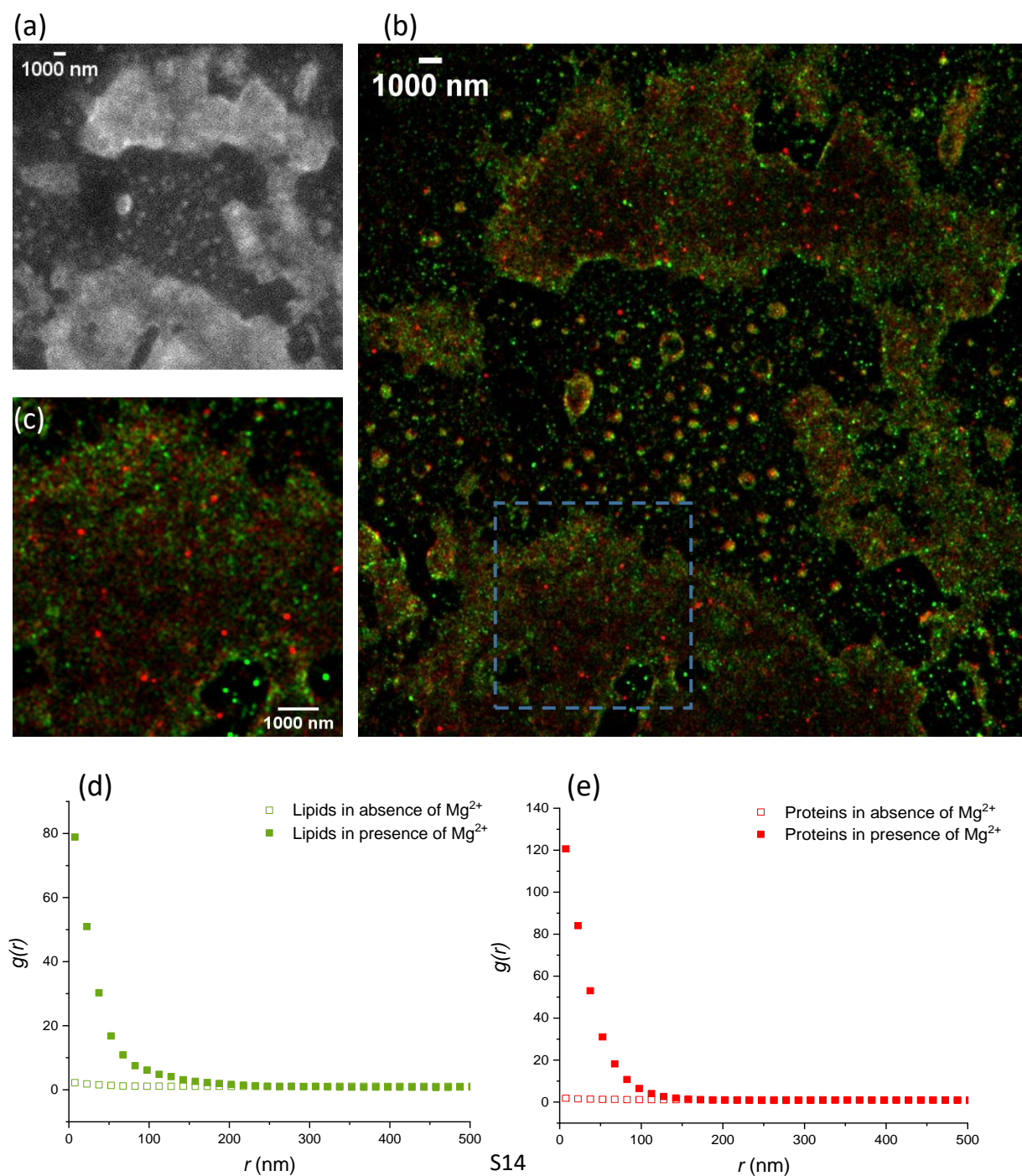


Figure S14. CLEM on the NR-SiO₂NPs composite labelling SiO₂NPs and proteins. (a) SE large view. (b) Magnified BSE image of the yellow boxed region in (b). (c) d-STORM micrographs of SiO₂NPs (cyan). (d) Dual color d-STORM micrographs combining the fluorescence signals of SiO₂NPs (cyan) and proteins (red), obtained with sequential acquisitions and recorded in the yellow boxed region of (a) showing the presence of proteins clusters in close proximity to structures of SiO₂NPs. (e) Cross-correlation analysis correlating the fluorescence signal of lipids with the one of SiO₂NPs, showing an increase of the pair correlation function $g(r)$ at distances <400 nm.

